ARTICLE

In-situ atomic force microscopic (AFM) investigation of kaolinite dissolution in high caustic environments

Received 00th January 20xx,
Accepted 00th January 20xx

DOI: 10.1039/x0xx00000x

Devalina Chaliha[c], Josè F. Gomes[a], Peter Smith[b], Franca Jones[a]*

Clays are a common component of bauxite and reactive silica, in the form of clays, is an important precursor of desilication products. Despite this, the behaviour or clays in highly caustic environments is not well investigated and this is due to the nature of the corrosive environment as well as the temperatures normally encountered (normally ~90°C for the desilication process unit). Atomic force microscopy has been used in this work to image the dissolution of kaolinite *in-situ* at various temperatures (25-55°C) and in different solutions (pure caustic, synthetic Bayer liquor and synthetic Bayer liquor with added waterglass). This work has shown that the dissolution behaviour is similar in all these solutions. Little impact of temperature is expected in the range studied though some of the results may be impacted by the batch nature of the set-up. In the synthetic Bayer liquor, due to aluminate present, it can also be concluded that the aluminate sheet of the kaolinite dissolves slower than the silicate sheet. The dissolution of kaolinite steps in Bayer liquor is slightly faster compared to the pure caustic case. In addition, there is a fast and slow dissolving direction for the steps observed on kaolinite. However, the size of the particle or features also change suggesting that edges are the fastest features to dissolve and this is supported by the initial formation of aluminosilicates at kaolinite edges.

Introduction,

The Bayer process is used worldwide for the refining of alumina (Al_2O_3) from bauxite ore. Bauxite consists mainly of gibbsite, boehmite and/or diaspore (aluminium (oxy) hydroxide minerals) as well as impurities such as silica minerals (including kaolinite and quartz).[1] The process involves mixing the crushed bauxite with caustic soda ($NaOH_{(aq)}$) to dissolve the aluminium-rich minerals. The concentrated caustic is heated at temperatures up to 270°C to completely dissolve these minerals.[2] A simplified representation of the process is shown in **Error! Reference source not found.**.

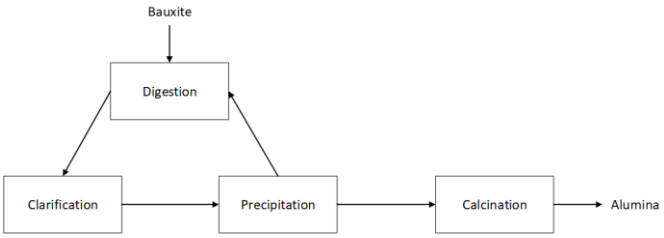

Figure 1. Schematic diagram of the Bayer Process

* *Corresponding author email: F.Jones@curtin.edu.au, phone 618 9266 7677*
a Curtin University, GPO Box U1897, Perth Australia, 6845
b Principal Consultant, Arriba Consulting, PO Box 75, Canning Bridge, Applecross, WA6153
c Curtin University, Department of Chemical Engineering
Electronic Supplementary Information (ESI) available: [showing sheet spacings, AFM images collected over time and temperature, additional analysis for width/heights of features and comparison of dissolution in Bayer and caustic solutions]. See DOI: 10.1039/x0xx00000x

The digested slurry is clarified to remove the insoluble residue ('mud') by filtration or settling. The mud is washed to recover caustic liquor, which is then recycled back to digestion. The filtrate liquor is precipitated by cooling and seeding, resulting in gibbsite solids ($Al(OH)_3$). After washing, the solids are calcined at very high temperatures to convert the gibbsite to anhydrous alumina (Al_2O_3).

Reactive silica includes silicates or clays that dissolve in the caustic conditions used and can cause unwanted side-reactions in the Bayer process.[2,3] The products that form from this dissolution are known as desilication products (DSPs) primarily formed during a pre-digestion step called pre-desilication.

An example of a dissolution reaction for kaolinite is shown in Equation 1.[4]

$$3Al_2Si_2O_5(OH)_4 + 18NaOH \rightarrow 6Na_2SiO_3 + 6NaAl(OH)_4 + 3H_2O \quad (Eqn.\ 1)$$

The dissolved silicate reacts with the sodium aluminate to form DSP, Equation 2.

$$6Na_2SiO_3 + 6NaAl(OH)_4 + Na_2X \rightarrow Na_6(Al_6Si_6O_{24})\cdot Na_2X + 12NaOH + 6H_2O \quad (Eqn.\ 2)$$

where X can be a variety of ions, the most important of which are CO_3^{2-} and SO_4^{2-}.[4] DSP can lead to scaling on tube walls and other processing equipment in the alumina plant. The situation is heightened at higher temperatures and hence, evaporator units and heat exchangers are often impacted by this issue.[5] Scaling ultimately reduces heat recovery efficiency and reduces

flow in equipment. In turn, these disruptions of liquor flow account for an increase in operating costs as well as requiring additional maintenance.[6-9] As seen in Equation 2, DSP formation also contributes to the loss of caustic soda.[10] Pre-desilication aims to lower silicate levels in the Bayer liquor by transforming the majority of the reactive silicas into DSP prior to digestion.[11,12]

DSP formation *can* involve several transition phases depending on the liquor composition and the source of silicate.[13-15] The final phases are either sodalite and cancrinite.[16] When kaolinite is present, sodalite is the only observed phase.[13,14,17]

There have been previous studies on kaolinite/clay dissolution using atomic force microscopy (AFM). The work of Sutheimer *et al.*,[18] is not directly comparable due to the use of acid conditions but their results confirmed that disordered kaolinite dissolved faster than more crystalline solids. Zbik and Smart[19] also used AFM to investigate kaolinite but this study was not in the presence of any solution and merely sought to understand the surface features and gross morphology of kaolinite. Other clays have been investigated, for example smectite[20] but different clays have different structures. Thus, there is no particular study that is directly comparable to the work presented here. Similarly, there is literature on the dissolution of kaolinite from other methods (such as[21]) but these are conducted at much lower pH where the aluminol groups are believed to be critical in the dissolution process. However, it is unclear whether this is also true at the high caustic concentrations encountered in the Bayer process (~5M).

Kaolinite is referred to as a 1:1 sheet silicate[22], with the formula $Al_2Si_2O_5(OH)_4$ ~~in which H_2O can be trapped in between the layers~~. It has the structure shown below (see supplementary information, SFig 1) consisting of alternating sheets of $Al(OH)_3$ octahedra and SiO_2 tetrahedra (the basal plane of kaolinite particles is the *c* axis) where they share a common plane of oxygens.[23]

It is stated that the octahedral sheet is ~0.51 nm while the tetrahedral sheet is ~0.21 nm[24] but this assumes that the interlayer water is associated with the octahedral sheet. In fact, the two sheets (octahedral and tetrahedral) are both ~0.2 nm in height. The step height of ~0.5 nm is, therefore, possible for both sheets (octahedral and tetrahedral) depending on which sheet is at the surface (see supplementary information, SFig 2) and is associated with the interlayer water.

In this work, atomic force microscopy (AFM), data was collected on kaolinite dissolution *in-situ* in the presence of caustic solution and Bayer liquor. Its behaviour was examined at various temperatures ranging from 20°C up to 55°C under caustic conditions that mimic the alumina refinery environment although the temperature is lower than that commonly found industrially (90°C). These changes through time can give more insight into kaolinite dissolution and which part of the structure is vulnerable to caustic attack.

Table 1 Elemental composition, expressed in terms of their %oxides, of the kaolinite and halloysite clays used in experiments (ref 17).

Chemical composition (% Oxides)	Al_2O_3	K_2O	Na_2O	SiO_2
	28.5	0.39	0.13	51.3
	Fe_2O_3	TiO_2	CaO	MgO
	1.51	0.32	0.04	N/A
Other properties				
Surface area^ m^2g^{-1}	15.50 ± _0.05			
Hinckley index	2.23			
Water* (wt%)	1.20			
Purity (wt%)	≥90			

*based on TGA mass loss
^based on BET

Methods and Materials

Kaolinite on mica prep:

Mica (1cm square) was peeled off a larger sample using tape. To prepare the kaolinite (Eckalite, English China Clay) the sample was slurried in water (3wt%) and, using a spin-coater (Laurell Technology Corporation, model: WS-400B-6NPP/LITE), was added drop wise onto the piece of mica to spread the sample across the surface of the mica (2000 rpm for 2 minutes). This sample of kaolinite has been previously characterised, ~~and the reader is referred to the following literature for details~~ (see refs 17, 25) but the properties are summarised in Table 1.

AFM conditions:

A Bruker 3100 AFM head was used for this investigation with the NanoScope (Bruker) software in contact mode. A DNP-A cantilever probe and Rev-D tip holder for fluids was used. The system incorporates a fluid cell with a Peltier heating stage. The dried kaolinite on mica was put into the holder and the solution added to the fluid cell at room temperature (see supplementary information, SFig 3 for a schematic). The AFM tip was engaged and an image taken to confirm the kaolinite clay is present. The tip was then disengaged and the temperature on the Peltier stage set to the required temperature (25°C initially). Once the system was equilibrated, the tip was re-engaged and imaging commenced. Waterglass (20 µL, 29.4wt% SiO_2, PQ Corporation - D Grade), if required, was added with a plastic syringe at 25°C prior to heating (the volume of the fluid cell was between 1-2 mL and this resulted in a final conc of SiO_2 0.05-0.1 g/L). When sufficient data had been collected the temperature was then raised to the next temperature. Finally, after all temperatures were investigated the system was allowed to cool to room temperature before everything was thoroughly cleaned and rinsed with water.

On obtaining the images from the AFM the following analysis was applied:
Using the height images large features were numbered and line scans were used to determine the height and width of each feature. In addition, atomic level steps and terraces were identified (see supplementary information, SFig 4) to obtain information regarding step dissolution rates and to try to identify whether there was preferential dissolution of a particular sheet (octahedral or tetrahedral). Deflection images were also collected to aid in the observation of steps and edges.

The solutions studied were: Caustic solution (5 mol/L NaOH), Synthetic Bayer liquor with total caustic of 4.7 mol/L NaOH and Al level equivalent to 0.73 mol/L Al_2O_3, and Synthetic Bayer liquor with waterglass added. All other parameters were as previously described. The liquor caustic and Al content was measured using the Connop[26] titration method.

For each system, the best series of images for analysis was selected; this decision was made based on the following criteria:

i) The particles were able to be monitored over the entire temperature range
ii) The particles contained sufficiently flat areas that could give step information
iii) The height images were of sufficient quality (noise and streaks) to be measured (for at least the majority of the temperatures)

As such, only one series per system was selected but the dissolution was observed to be similar even in those systems not fully analysed. In terms of variability, the greatest source of error comes in the measurement of the steps and terraces. The choice of where the measurement starts and stops becomes critical. This has been conservatively estimated to be ±10%.

The maximum reaction temperature was 55 °C due to the following considerations: the first contact of the clay/bauxite with the caustic solution occurs at much lower temperature than 90 °C in the mills, limitation of the experimental set up - evaporation issues and the AFM tip dissolving at higher temperatures, bubble formation occurred over time (interferes with correct contact with the surface and obscures surface textures of the clay), higher temperatures could lead to dissolution that could be too fast to follow.

Silicate solubility versus temperature

In order to properly assess the impact of temperature on the dissolution of kaolinite, it is important to at least have some feel for how much silicate is expected to be soluble in caustic/Bayer liquor in the range 25-55 °C. To that end, the correlations of Breuer et al.,[27] were used to determine the silica concentration at 250 g/L NaOH, 75 g/L alumina and at temperatures ranging from 25-55°C. Using these relationships, the dissolved silica concentration would be expected to be approximately $[SiO_2]$ = 0.1 – 0.2 g/L and the impact of temperature is expected to be negligible. The main parameter determining the *amount* of kaolinite dissolution is the free caustic concentration (from bulk studies[28]). Since temperature has a minimal impact on the equilibrium solubility of kaolinite it can be assumed that temperature will only impact the kinetics of dissolution in this closed (batch-like) system. Also, from Benezeth et al.,[29] the solubility of aluminate was calculated where it was found that at 55°C the concentration of aluminate in the Bayer liquor is actually supersaturated, however, gibbsite precipitation is notoriously slow[30] particularly at the temperatures investigated here and is not expected to be observed.

Results and discussion

Pure caustic

Particles that were reasonably flat were chosen to maximise the possibility of imaging step dissolution. An example of such a particle is shown in Figure 2. Features on this particle were numbered and their height monitored over the course of the experiment. In addition, as can be seen in the supplementary information (Figure S5), a step edge was also observed. In this instance the length of the terrace width (see Figure S4) as the step dissolved away was also measured and monitored with temperature changes.

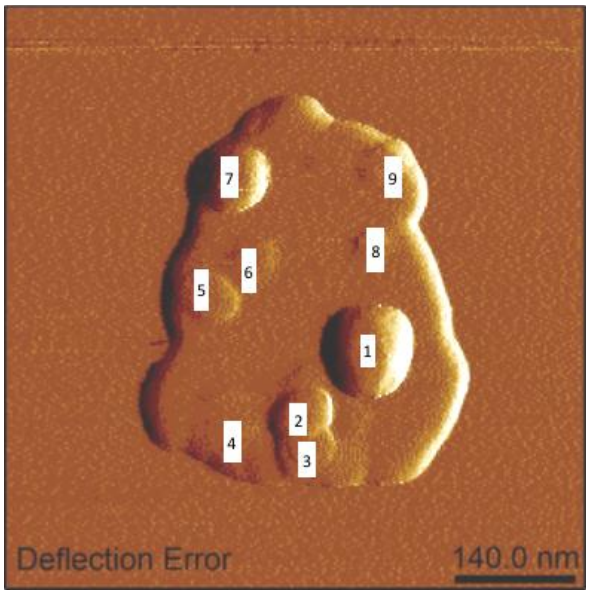

Figure 2. Kaolinite particle monitored over time with features numbered

It was found that the terrace width (and therefore step dissolution) increased with temperature until 45°C (see Figure 3). The rate of step dissolution was not significantly different between 45 and 55°C. Little to no trend in silica solubility is expected within the temperature range tested so it is possible that the equilibrium solubility of silicate in the caustic solution is already reached before the temperature is further raised, meaning that dissolution is already significantly slowed by the

time the data at 55°C is collected (due to the liquid cell being a closed system). It is also possible that the atomic composition of the sheet dissolving at 45°C is not the same as that dissolving at 55°C and therefore it has a different dissolution rate[31-33].

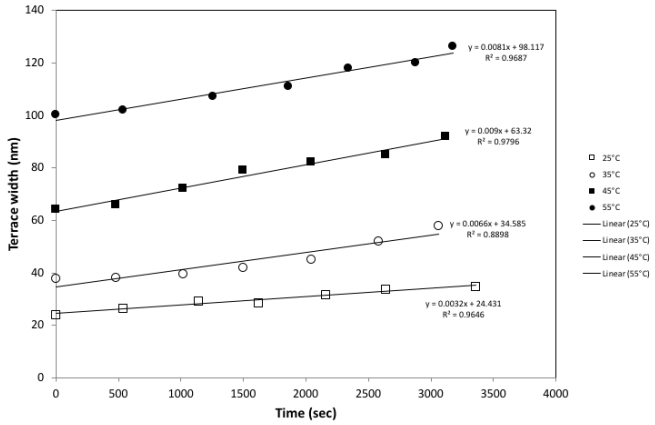

Figure 3. Step ledge size (at different temperatures) versus time

The step height of this feature remained in the 0.51-0.59 nm range (see supplementary information, Figure S5b) and the flat plane is assumed to be the *c* axis of the kaolinite structure. While the tetrahedral sheet has been stated to have a thickness of 0.21 nm and the octahedral sheet a thickness 0.51 nm,[24] as mentioned previously this may not be correct. If the Al octahedral sheet is preferentially dissolved, this may be rationalized by the fact that the octahedral sheets are where the hydroxyls are bonded. In addition, the rate-limiting step according to Huertas et al.[31], is the formation of the $>AlO^-$ surface complex (in alkaline solution). Studies suggest that the contribution of the basal plane to the dissolution rates is critical, as it provides the structural hydroxyls to be deprotonated and form the surface complexes[31-33]. However, some of this work was conducted at <1 M caustic and as such may not be applicable to Bayer-like conditions (≥5 M). Additionally, this conclusion was made on the basis of solution species or modelling of the basal faces and not on particle measurements so it is possible the importance of edges may have been missed.

In monitoring the features on the kaolinite particle, it was observed that there was a cyclic nature to the dissolution between temperatures. The features sometimes dissolving slowly and then at other times dissolving more quickly (see lines drawn in Figure 4). One possible reason for this is that the system is equilibrated with respect to dissolved silicate by the time the temperature is raised from say 35°C to 45°C but on further increases in temperature (say to 55°C) a new equilibrium is established. However, as the temperature is unlikely to change the equilibrium silicate level this hypothesis can be discarded.

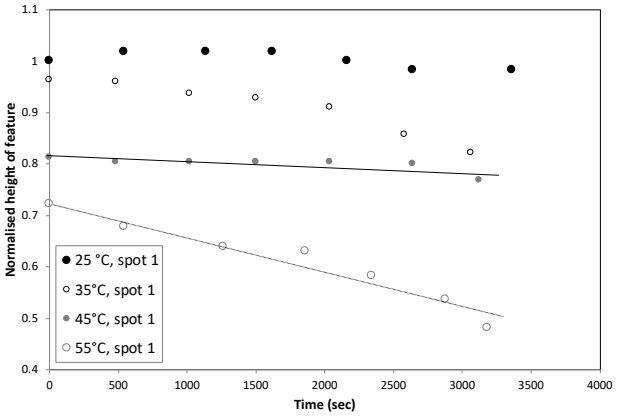

Figure 4. Normalised height (height at time, t, divided by height at t_o) versus time for 'spot 1' shown in Figure 5 at different temperatures

While the heights have been normalized to make comparison easier, the heights dissolved are in the nm range and therefore represent several kaolinite *c*-layer thicknesses (see supplementary information, Figure S6). Thus, a more plausible explanation is that the structure includes slower dissolving features and depending on which features are exposed to the liquor different dissolution rates will be observed. If the steepest curve is used to calculate a rate of dissolution (55°C gives a slope of $-4x10^{-4}$ nm/s) for this feature, these rates are much less than that for the step dissolution ($8x10^{-2}$ nm/s). This is because the two are not strictly comparable - Figure 3 represents a purely lateral dissolution rate (terrace width changes) while Figure 4 represents both a lateral and a vertical dissolution rate (because the height can only decrease once the step has dissolved). What is of additional interest in analyzing the changes in spot 1 is that the width of the spot reduces more than its height (8.0 versus 3.3 nm, see Figure S6 in the supplementary information) over the same time period. This suggests while kaolinite can dissolve through steps, step edges are more important.

One final interesting note is that the left side step of this particle appears to be dissolving more than the right side step (in fact there is no equivalent right side step). This could imply that the step is not symmetrical in the positive and negative direction akin to the obtuse and acute step (<441>, step directions) of calcite.[34] Stadler and Schindler[35] proposed that smectite dissolution under alkaline conditions was related to the number of charged aluminol groups (>AlO–) located on the edges of the clay structure and this is similar to that found for kaolinite but for the basal plane[31-33]. In the case of the smectite and kaolinite clay, the detachment of aluminate was the rate-limiting step for the dissolution reaction.[21,31-33,36,37]

Bayer liquor

All of the comments made with respect to dissolution in pure caustic are also seen in synthetic Bayer liquor. The measurement of the terrace width was not possible at 55°C due

to the quality of the AFM height images. However, comparison of Figure 3 to Figure 5 reveals the rates of dissolution for steps are marginally greater in Bayer liquor than in caustic despite the slight *decrease* in free caustic. In addition, as per the caustic situation, the rate of dissolution at the higher temperature was slower than at the lower temperature. In this case dissolution at 45°C is found to be slower than at 35°C. The same possibilities as were discussed in pure caustic apply here as to why this may be. Direct comparison of the temperature impacts can also be found in the supplementary information (see Figure S7).

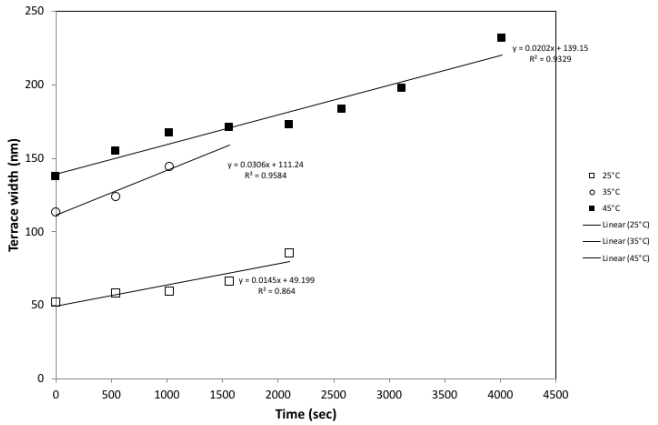

Figure 5. Step ledge size versus time in Bayer liquor at different temperatures

As found for the caustic case, there are slow and fast periods in the dissolution of the clay particle (see Figure 6 for the particle monitored). In the presence of synthetic Bayer liquor, the change from slow to fast dissolution can be found within a given set temperature of data collection as well as between temperatures (see Figure 7). Deflection images at the different temperatures can be found in the supplementary information, (Figure S8).

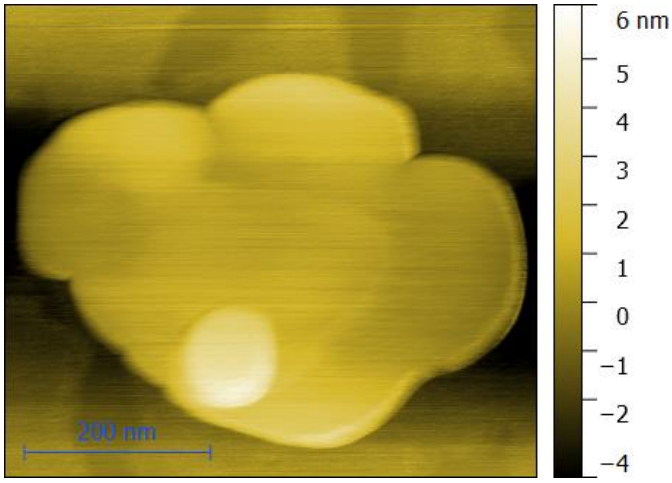

Figure 6. Kaolinite particle monitored in Bayer liquor over time and different temperatures, a feature labelled 1n is also shown

The steepest slope of the curves in Figure 7 corresponds to -6x10^{-4} nm/s at 35 °C. This suggests that the dissolution is similar to features in pure caustic if the maximum rate of dissolution is compared (c/f -4x10^{-4} nm/s in pure caustic). While the free caustic in Bayer liquor is lower than that in pure caustic[28], the rate at which the kaolinite dissolves may not be linked to the degree of understaturation. In addition, in this Bayer liquor the system is supersaturated with respect to aluminate (no driving force for dissolution of aluminate sheets) so it is unexpected that the dissolution is similar in both situations. The high rate of dissolution in Bayer liquor, however, suggests that the Benezeth et al.,[29] relationship may not hold under these conditions and that aluminate is still dissolving. Or, it could be that silanol groups perhaps also dissolve appreciably and contribute to the dissolution rate under Bayer-like conditions. As with the dissolution in pure caustic, the direction of the step is also important with one direction dissolving much faster than the other (in Figure 9 the right-hand side of the step is the faster dissolving direction). Thus, the step will have an average dissolution rate that is a combination of the fast and slow direction. Finally, it should be stressed that the edges of the kaolinite particle are attacked in preference to sites on the terrace (flat surface) or steps thus suggesting that regardless of the sheet it is the defective edges that dominate the process of dissolution as found for the pure caustic case.

Dissolution in the presence of additional silicate

Another experimental condition tested was the dissolution of kaolinite in the presence of synthetic Bayer liquor but with additional waterglass added. These experiments were conducted at a single temperature 55°C and investigated how dissolution occurred when additional silicate is present. The behaviour of the kaolinite was found to be the same as previously observed and the dissolution of the particles both through dissolution of steps and through attack at the edges can be seen, this is despite the additional silicate concentration present (and therefore the smaller driving force for dissolution of either aluminate or silicate sheets).

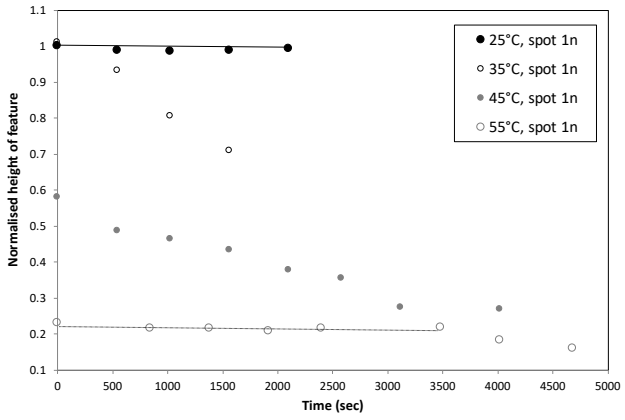

Figure 7. Normalised height versus time for 'spot 1n' shown in Figure 10 in Bayer liquor at different temperatures

To show how significant dissolution through the attack at edges can be Figure 8 shows a region with kaolinite particles initially and after 121 minutes. For one of these particles, line profiles are shown.

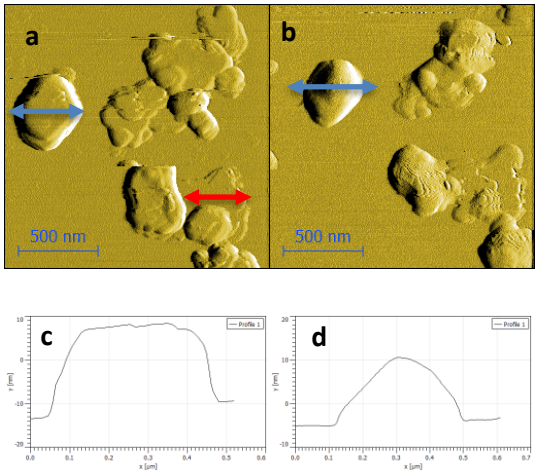

Figure 8. Deflection AFM images of region at a) 12:11 pm and b) 14:12 pm. The line profiles below correspond to the blue double-sided arrow section above

Initially the particle shown in Figure 8 with the blue arrow is ~21.0 nm high and 434.0 nm wide. After 2 hours the particle is ~15.0 nm high and 378.0 nm wide. Thus, while the height changed by 7.0 nm the width shrunk by 56.0 nm. The deflection images can be found in the supplementary section (Figure S9). What is perhaps more interesting is to see what happens to the feature shown by the red double-headed arrow. This region consists of steps, initially multiple unit cells high (in the *c* direction) as shown by the line profile in Figure 9a.

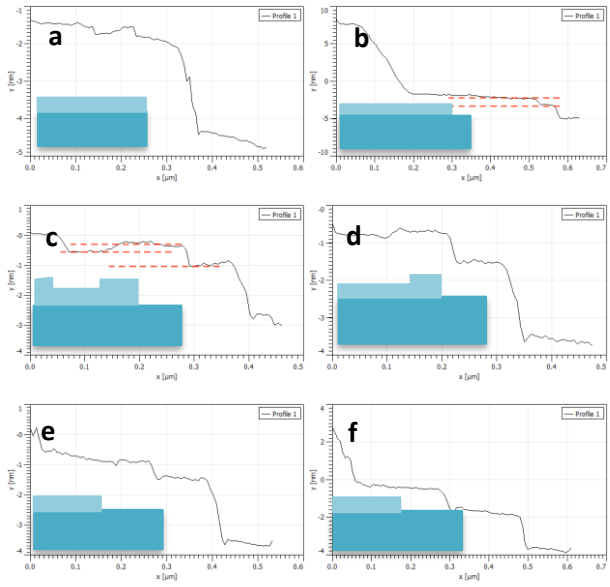

Figure 9. The line profile corresponding to the red double-sided arrow section in Figure 8 (a) at 12:11pm, (b) 12:52pm, (c) 13:32pm, (d) 13:46pm, (e) 14:03pm, (f) 14:12pm. The schematic insert represents the dissolution of the top sheet (light blue) from the bottom 'bulk' section (darker blue shade)

As the step dissolves, a new step appears that is ~0.8 nm high. This feature is slow moving and persists, but a new feature develops on the other side that is ~0.3 nm high. This suggests that a dissolution etch pit is formed (most probably through a defect site). This step feature becomes smaller and smaller until it disappears, and the step goes from being ~0.8 to ~0.6 nm. In addition, the persistence of the step beneath the dissolving one (without the appearance of a new step), confirms that there are fast dissolving steps and slower dissolving steps. Finally, the dissolution from one side of the etch pit being faster than the other confirms that there is a preferred dissolution direction.

The question becomes whether any of these smaller step heights (0.5-0.6 nm) and (~0.3 nm) can be assigned to any particular sheet (octahedral or tetrahedral). Given that this is in a Bayer liquor that is supersaturated with aluminate but slightly undersaturated with respect to silicate – it is hypothesized that the tetrahedral (silicate) sheet is the fast dissolving 0.3 nm step while the aluminate sheet is slower dissolving. However, this may not be the case if the aluminate is not as supersaturated as calculated and may be different in pure caustic where the aluminate level is lower.

The results shown here with AFM are supported by the work of N'guessan *et al.*[38]. While the work from this group involved investigation at lower concentrations (2 M) of caustic solutions it also included potassium hydroxide. Their work showed that sodium ions were more potent in dissolving the kaolinite and that terraces dissolved through etch pits (presumably through attack at defects). While this may seem to contradict the results here, in fact, they do not. AFM results not displayed here in potassium hydroxide showed little impact at 25 °C which lead us to switch to sodium hydroxide. Thus, the lesser impact of potassium hydroxide is supported. Also, without being able to monitor individual particles, it is difficult to see that edges are also being attacked. This is one benefit of the AFM technique. Finally, as seen in the Bayer liquor system with waterglass added, etch pits can and do form and so the work presented here is consistent with the data on kaolinite dissolution from this work, keeping in mind that the AFM highlights the early stages of the dissolution process.

These *in-situ* AFM results are also supported by Gomes et al.,[17] showing that the initial formation of DSP particles are mostly at the edges of kaolinite particles ~~(Figure 13)~~. This suggests a local supersaturation with respect to DSP could be formed in this region, promoting the heterogenous nucleation of DSP particles.

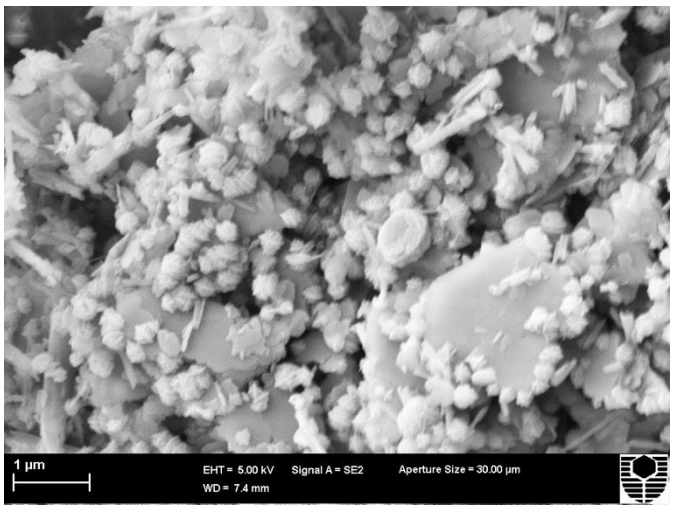

Figure 13. SEM image of DSP formed on kaolinite particles (reproduced with permission from ref 17)

Conclusions

In this study, AFM was used to image the dissolution of kaolinite *in-situ* at various temperatures (25-55°C). This work has shown that the overall dissolution behaviour is similar for the different solutions; be it pure caustic, synthetic Bayer liquor or synthetic Bayer liquor with added waterglass.

It was observed that the kaolinite dissolves mainly from the edges, with the width of kaolinite particles reducing at a much greater rate than their heights. The dissolving steps were seen to be ~ 0.5 nm in height but this could not be definitively attributed to either the tetrahedral or octahedral sheet. In pure caustic, this could suggest preferential dissolution of the octahedral sheet but in Bayer liquor this would be less likely (due to the liquor being supersaturated with respect to aluminate). This suggests that in Bayer liquor (and perhaps also in high caustic concentrations) silanol groups may also be important in the dissolution process. The dissolution of steps generally increased with temperature but dissolution of kaolinite in Bayer liquor did not follow the expected trend from a free caustic perspective. Finally, there appears to be a fast and slow dissolving direction for the step.

On addition of waterglass to the system and maintaining temperature at 55°C, a fast dissolving step at ~0.3 nm was observed that was not observed in the other two systems. Due to the properties of the liquor, it is hypothesized that this sheet is the silicate sheet.

To conclude, this work shows that AFM can be used in challenging environments and that there is much still to learn about clays and their behaviour in caustic environments. In particular, there is much scope to learn which of the sheets, if any, preferentially dissolves under which conditions and whether this alters with clay type.

Author Contributions

DC conducted AFM experiments, FJ conceptualized the work and wrote the first draft. All authors contributed to scientific analysis and writing of the final draft.

Conflicts of interest

There are no conflicts of interest to declare. Funding from AQW and the Australian government is acknowledged in supporting J Gomes.

Acknowledgements

We would like to acknowledge and thank Dr. Thomas Becker, Curtin University for his help with the AFM (training and equipment). Similarly, we would like to acknowledge the John de Laeter Centre, Curtin University for use of the electron microscope facility (ARC LE130100053, LE140100150, LE0775551). Finally, we would like to acknowledge the AQW (Alumina Quality Workshop) and Curtin University for J. Gomes' Australian postgraduate award.

References

1 Zeng, L.; and Li, Z. (2012) "Solubility and Modeling of Sodium Aluminosilicate in NaOH–NaAl(OH)$_4$ Solutions and Its Application to Desilication" *Industrial & Engineering Chemistry Research,* **51(46)**, 15193-15206.

2 Authier-Martin, M.; Forte, G.; Ostap, S.; and See, J. (2001) "The Mineralogy of Bauxite for Producing Smelter-Grade Alumina" *JOM,* **53(12)**, 36- 40.

3 Jamialahmadi, M.; and Müller-Steinhagen, H. (1998) "Determining Silica Solubility in Bayer Process Liquor" *JOM,* **50(11)**, 44-49.

4 Smith, P. (2009) "The Processing of High Silica Bauxites — Review of Existing and Potential Processes" *Hydrometallurgy,* **98(1)**, 162-176.

5 Ulmgren, P. (1982) "Consequences of Build-up of Non-Process Chemical Elements in Closed Cycle Kraft Recovery Cycles-Aluminosilicate Scaling, a Chemical Model" *CPPA/TAPPI Int. Conf.(Vancouver) Recovery Pulping Chemicals*.

6 Barnes, M. C.; Addai-Mensah, J.; and Gerson, A. R. (1999) "The Solubility of Sodalite and Cancrinite in Synthetic Spent Bayer Liquor" *Colloids and Surfaces A: Physicochemical and Engineering Aspects,* **157(1-3)**, 101-116.

7 Barnes, M. C.; Addai-Mensah, J; and Gerson A. R. (1999) "The Kinetics of Desilication of Synthetic Spent Bayer Liquor and Sodalite Crystal Growth." *Colloids and Surfaces A: Physicochemical and Engineering Aspects,* **147(3)**, 283-295.

8 Barnes, M. C.; Addai-Mensah, J; and Gerson A. R. (1999) "The Kinetics of Desilication of Synthetic Spent Bayer Liquor Seeded with Cancrinite and Cancrinite/Sodalite Mixed-Phase Crystals." *Journal of Crystal Growth,* **200(1-2)**, 251-264.

9 Barnes, M. C.; Addai-Mensah, J; and Gerson A. R. (1999) "The Mechanism of the Sodalite-to-Cancrinite Phase Transformation in Synthetic Spent Bayer Liquor." *Microporous and Mesoporous Materials,* **31(3)**, 287-302.

10 Croker, D.; Loan, M.; and Hodnett, B. K. (2008) "Desilication Reactions at Digestion Conditions: An *in situ* X-Ray Diffraction Study." *Crystal Growth & Design,* **8(12)**, 4499-4505.

11 Whittington, B. I.; Fletcher, B. L.; and Talbot, C. (1998) "The Effect of Reaction Conditions on the Composition of Desilication Product (DSP) Formed under Simulated Bayer Conditions." *Hydrometallurgy,* **49(1-2)**; 1-22.

12 Whittington, B. I.; and Fallows, T. (1997) "Formation of Lime-Containing Desilication Product (DSP) in the Bayer Process: Factors Influencing the Laboratory Modelling of DSP Formation." *Hydrometallurgy,* **45(3)**; 289-303.

13 Peng, H; Ding, M; and Vaughan, J. (2018) "The anion effect on Zeolite Linde Type A to sodalite phase transformation" *Industrial & Engineering Chemistry Research*, **57(31)**, 10292-10302.

14 Radomirovic, T.; Smith, P.; Southam, D.; Tashi, S; and Jones, F. (2013) "Crystallization of Sodalite Particles under Bayer-Type Conditions." *Hydrometallurgy,* **137**; 84-91.

15 Smith, P. G., Lowe, J. L., Rohl, A. L, Pennifold, R. M. and Parkinson, G. M., 2002. "Understanding growth of DSP in the presence of inorganic ions" Proceedings of the 6th International Alumina Quality Workshop, Brisbane, Queensland, 191-194. http://hdl.handle.net/102.100.100/199209?index=1

16 Zeng, L.; and Li, Z. (2012) "Solubility and Modeling of Sodium Aluminosilicate in NaOH–$NaAl(OH)_4$ Solutions and Its Application to Desilication" *Industrial & Engineering Chemistry Research,* **51(46)**, 15193-15206.

17 Gomes, J. F.; Davies, M.; Smith, P. and Jones, F. (2021) "The formation of desilication products in the presence of kaolinite and halloysite – the role of surface area" *Hydrometallurgy*, **203**,105643-105655.

18 Sutheimer, S. H.; Maurice, P. A.; and Zhou, Q. (1999) "Dissolution of well and poorly crystallized kaolinite: Al speciation and effects of surface characteristics" *American Mineralogist*, **84**, 620–628.

19 Zbik, M.; and Smart; R. St. C. (1998) "Nanomorphology of Kaolinites: Comparative SEM and AFM Studies" *Clays and clay Minerals,* **46(2)**; 153-160.

20 Kuwahara, Y. (2006) "In-situ AFM study of smectite dissolution under alkaline conditions at room temperature" *American Mineralogist,* **91**, 1142–1149.

21 Huertas, F.J.; Chou, L.; and Wollast, R. (1999) "Mechanism of kaolinite dissolution at room temperature and pressure Part II: Kinetic study" *Geochimica et Cosmochimica Acta*, **63**, 3261–3275.

22 Weck, P. F.; Kim, E.; and Jové-Colón (2015) "Relationship between crystal structure and thermomechanical properties of kaolinite clay: beyond standard density functional theory" *Dalton Transactions*, **44**, 12550-12560.

23 Zhang, S.; Liu, Q.; Gao, F.; Li, X.; Liu, C.; Li, H.; Boyd, S. A.; Johnston, C. T.; and Teppen, B. J (2017) "Mechanism associated with kaolinite intercalation with urea: Combination of infrared spectroscopy and molecular dynamics simulation studies" *J. Phys. Chem. C.*, **121**, 402-409.

24 Sachan, A.; and Penumadu, D. (2007) "Identification of Microfabric of Kaolinite Clay Mineral Using X-Ray Diffraction Technique." *Geotechnical and Geological Engineering,* **25(6)**; 603-616.

25 Radomirovic, T.; Smith, P.; and Jones, F. (2013) "Using Absorbance as a Measure of Turbidity in Highly Caustic Solutions." *International Journal of Mineral Processing,* **118**; 59-64.

26 Connop, W. L., (1996) "A new procedure for the determination of alumina, caustic and carbonate in Bayer liquors" Fourth International Alumina Quality Workshop, pp. 321–330.

27 Breuer, R.G., Barsotti, L.R. and Kelly, A.C. (1963) "Behaviour of silica in sodium aluminate solutions": in "The extractive metallurgy of aluminium" pp133-157. Eds. Gerard, G. and Stroup, P.T. Interscience New York.

28 Gräfe, M.; Klauber, C.; McFarlane, A. J. and Robinson, D. J. eds (2017) "Clays in the Mineral Processing Value Chain", Cambridge University Press pp122.

29 Bénézeth, P.; Hilic, S.; and Palmer, D. A. (2016) "The Solubilities of Gibbsite and Bayerite Below 100 _C in Near Neutral to Basic Solutions" *J Solution Chem* **45**:1288–1302.

30 Loh, J. S. Fogg, A. M., Watling, H. R., Parkinson, G. M. and O'Hare, D (2000) "A kinetic investigation of gibbsite precipitation using *in situ* time resolved energy dispersive X-ray diffraction" *Phys. Chem. Chem. Phys.*, **2**, 3597-3604.

31 Huertas, F. J.; Chou, L.; Wollast. R. (1998) "Mechanism of Kaolinite Dissolution at Room Temperature and Pressure: Part 1. Surface Speciation", *Geochimica et Cosmochimica Acta*, **62(3)**, 417-431.

32 Khorshidi, Z. N.; ; Tan, X.; Liu, Q.; and Choi, P. (2018)"Molecular dynamics study of the dissolution mechanism of kaolinite basal surfaces in alkali media", *Applied Clay Science*, **152**, 29-37.

33 Bauer, A.; and Berger,G. (1998) "Kaolinite and smectite dissolution rate in high molar KOH solutions at 35° and 80°C", *Applied Geochemistry*, **13(7)**, 905-916

34 De La Pierre, M.; Raiteri, P.; Gale, J. D. (2016) "Structure and dynamics of water at step edges on the calcite {1014} surface" *Cryst. Growth Des.*, **16(10)**, 5907-5914.

35 Stadler, M.; and Schindler, P.W. (1993) "Modeling of H+ and Cu2+ adsorption on calcium-montmorillonite" *Clays and Clay Minerals*, **41**, 288–296.

36 Devidal, J.L.; Schott, J.; and Dandurand, J.L. (1997) "An experimental study of kaolinite dissolution and precipitation kinetics as a function of chemical affinity and solution composition at 150 °C, 40 bars, and pH 2, 6.8, and 7.8" *Geochimica et Cosmochimica Acta*, **61**, 5165–5186.

37 Huertas, F.J.; Caballero, E.; Jiménez de Cisneros C.; Huertas, F.; and Linares, J. (2001) "Kinetics of montmorillonite dissolution in granitic solutions" *Applied Geochemistry*, **16**, 397–407.

38 N'Guessan, N. E.; Joussein, E.; Courtin-Nomade, A.; Paineau, E.; Soubrand, M.; Grauby, O.; Robin, V.; Cristina, C. D.; Vantelon, D.; Launois, P.; Fondanèch, P.; Rossignol, S.; Texier-Mandoki, N.; and Bourbon, X. (2021) "Role of cations on the dissolution mechanism of kaolinite in high alkaline media", *Applied Clay Science*, **205**, 106037-106049.